ELSEVIER

Journal of Alloys and Compounds 330–332 (2002) 861–865

Journal of ALLOYS AND COMPOUNDS

www.elsevier.com/locate/jallcom

# Influence of the material processing on the electrochemical properties of cobalt-free Ml(NiMnAlFe)$_5$ alloy

Y.Q. Lei[a,*], S.K. Zhang[a], G.L. Lü[b], L.X. Chen[a], Q.D. Wang[a], F. Wu[c]

[a]*Department of Materials Science and Engineering, Zhejiang University, Hangzhou, 310027, PR China*
[b]*Central Laboratory, Zhejiang University, Hangzhou, 310028, PR China*
[c]*National Engineering Development Center of High Technology Energy-storage Materials, Zhongshan, 528437, PR China*

**Abstract**

Co-free MlNi$_{4.1}$Mn$_{0.35}$Al$_{0.3}$Fe$_{0.25}$ (Ml: La-rich mischmetal) alloy samples were prepared in three different ways. The original as-cast alloy was prepared by vacuum levitation melting in a cold crucible. One-third of the as-cast ingot was annealed at 1273 K for 10 h, and another one-third was remelted and rapidly solidified by melt-spinning. The influence of the alloy preparation methods on their microstructure and electrochemical properties was studied. XRD and SEM results revealed that all of the three differently prepared alloys were of the single CaCu$_5$-type structure phase, but their microstructure and electrochemical properties were changed markedly. The as-cast alloy had a typical dendrite structure with noticeable composition segregation and rather poor cycling endurance. While the annealed and melt-spun alloy were of an equiaxed structure and a very fine cellular structure, respectively, and had a more homogeneous composition and dramatically improved cycling endurance, although their activation rate and high-rate dischargeability were lowered somewhat. In this study, the melt-spun Co-free alloy showed the best cycling stability ($S_{500}$=69.2%) and a reasonably high capacity (305 mA h g$^{-1}$) and 1C rate dischargeability (85.6%), which is attributed to its lower degree of pulverization and more uniform composition.


*Keywords:* Hydrogen storage alloy; Cobalt-free alloy; Material processing; Microstructure; Electrochemical property

## 1. Introduction

Mischmetal-based AB$_5$-type alloys containing about 10 wt.% Co are now widely used as the negative electrode material of Ni/MH batteries because of their long cycle life and good overall properties. However, since cobalt is the most expensive element in the commercial AB$_5$ alloys, in order to reduce the alloy cost, the substitution of expensive cobalt with other low-cost elements is very desirable. So far, some elements, including Cu, Fe, Si, Cr, Sn, etc. have been used for cobalt substitution and several low-Co or Co-free alloys have been developed [1–7]. It is found that alloys without cobalt or with low cobalt contents generally have a much shorter cycle life compared to the high-Co (10% Co) alloys. Meanwhile, it has been found that the microstructural homogeneity and electrochemical cycling stability of the mischmetal-based alloys with different Co contents can be improved by different material processing methods such as heat treatment [2,4,9,10] and rapid solidification including gas atomizing [5,6] and rapid quenching [7–11]. However, it appears to us that the influence of alloy composition and preparation methods on the cycling performance is quite complex and is as yet not very clear. In addition, for the Co-free Fe-containing alloys, no detailed information on the effects of the rapid quenching process on the microstructure and electrochemical properties is available in the literature.

In this work, the influence of annealing treatment and rapid quenching of the Co-free MlNi$_{4.1}$Mn$_{0.35}$Al$_{0.3}$Fe$_{0.25}$ alloy on the microstructure and electrochemical properties is investigated.

## 2. Experimental details

MlNi$_{4.1}$Mn$_{0.35}$Al$_{0.3}$Fe$_{0.25}$ alloy samples (Ml: La-rich mischmetal with the composition of 54.7 wt.% La, 29.5 wt.% Ce, 12 wt.% Pr, 3.5 wt.% Nd and 0.3 wt.% impurity, and all starting elemental metals have a purity higher than 99.9%) were prepared by vacuum levitation melting in argon atmosphere and remelted three times to ensure a high homogeneity. One-third of the as-cast ingot was annealed under vacuum at 1273 K for 10 h. Another one-third of the as-cast ingot was remelted and quenched

*Corresponding author.

0925-8388/02/$ – see front matter 
PII: S0925-8388(01)01483-9

by melt-spinning method. The linear velocity of the rotating molybdenum roller used for the rapid quenching process was 15 m $s^{-1}$.

The alloy samples thus prepared were ground mechanically into powder below 300 mesh and used for electrochemical measurements and X-ray diffraction (XRD) analysis. For the electrochemical measurements, the alloy powder (about 100 mg) was mixed with electrolytic copper powder (44 μm) in a mass ratio of 1:2 and cold pressed to an electrode pellet ($d$=10 mm). Electrochemical measurements were carried out at 25°C in a tri-electrode half cell with $Ni(OH)_2$/NiOOH as the counter electrode and Hg/HgO as the reference electrode, in a 6 M KOH electrolyte. The electrode activation and test for maximum capacity $C_{max}$ were carried out at the charge–discharge current of 50 mA $g^{-1}$ with 8 h for charging and the cut-off voltage of −0.6 V (vs. Hg/HgO) for discharging. The high rate dischargeability (%), defined as $C_n \times 100/(C_n + C_{50})$, was determined from the ratio of the discharge capacity $C_n$ (with $n$=300, 600 or 900 mA $g^{-1}$, respectively) to the total discharge capacity defined as the sum of $C_n$ and $C_{50}$, which was the additional capacity measured subsequently at 50 mA $g^{-1}$ after $C_n$ was measured. The cycling test was conducted at the charge–discharge current of 300 mA $g^{-1}$. The cycling capacity retention rate $S_{300}$ and $S_{500}$ were defined as $S_{300}(\%) = C_{300} \times 100/C_{max}$ and $S_{500} = C_{500} \times 100/C_{max}$, where $C_{300}$ and $C_{500}$ were the discharge capacities at $300^{th}$ and $500^{th}$ cycles, respectively.

The phase structure of the samples was determined by XRD analysis using a Rikagu D/Max-313 X-ray diffractometer with Cu Kα radiation. The continuous scanning speed was 4° $min^{-1}$, and the $2\theta$ range was 20–90°. The results were analyzed by the Rietveld method. The microstructure and the composition of the samples were examined using a Philips-XL30 scanning electron microscope (SEM) and EDS.

## 3. Results and discussion

### 3.1. XRD analysis

Fig. 1 shows the XRD patterns of the $MlNi_{4.1}Mn_{0.35}Al_{0.3}Fe_{0.25}$ alloy prepared by three different methods. The three differently prepared alloys had nearly the same pattern except for a small difference in intensity. They were all indexed as the single phase $CaCu_5$-type structure. In addition, the diffraction peaks for $CaCu_5$-type phase become narrower and sharper after annealing and rapid quenching treatment, indicating that both the annealed and the melt-spun alloy have a higher crystallinity and relaxed lattice strain.

The lattice parameters and Rietveld analysis results of the microstructure parameters for the three differently prepared alloys are listed in Table 1. Compared to the

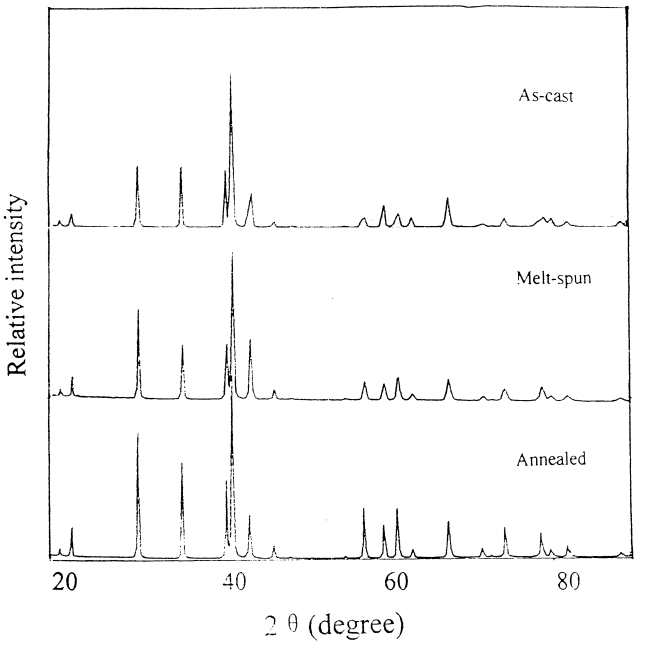


Fig. 1. The XRD patterns of $MlNi_{4.1}Mn_{0.35}Al_{0.3}Fe_{0.25}$ alloys prepared by three different methods.

lattice parameters of the as-cast alloy, the $a$-axis of the annealed alloy becomes smaller and the $c$-axis becomes longer, while both the $a$-axis and the $c$-axis of the melt-spun alloy become longer. From Table 1, it can also be seen that the crystallite size $M_{nn}$ (in all three dimensions) of the alloys is greatly changed in accordance with preparation methods. For the as-cast alloy, the crystallite size is about 60 nm in $a$- and $b$-axis directions and 25 nm in the $c$-axis direction, but that of the annealed alloy is much larger and about 112 nm in $a$- and $b$-axis directions and 249 nm in $c$-axis direction. The crystallite size of the melt-spun alloy is also slightly larger than that of as-cast alloy with the same dimension (62–63 nm) in all directions. These results indicate that the crystallite shape and

Table 1
The lattice parameters, crystallite size and micro-strain of $MlNi_{4.1}Mn_{0.35}Al_{0.3}Fe_{0.25}$ alloys

| Parameter | As-cast | Annealed | Melt-spun |
|---|---|---|---|
| $a$ (nm) | 5.0093 (9) | 5.0068 (3) | 5.0122 (3) |
| $c$ (nm) | 4.0552 (5) | 4.0663 (2) | 4.0633 (2) |
| $M_{11,22}$ (nm) | 60.24 (0.37) | 111.64 (0.52) | 62.10 (0.31) |
| $\langle \epsilon^2 \rangle^{1/2}_{11,22}$ | 0.0018 | 0.0007 | 0.0006 |
| $M_{33}$ (nm) | 24.74 (0.17) | 248.51 (0.75) | 63.18 (0.29) |
| $\langle \epsilon^2 \rangle^{1/2}_{33}$ | 0.0020 | 0.0002 | 0.0011 |
| $R_{wp}$ | 21.22 | 18.67 | 9.60 |
| $R_p$ | 16.45 | 14.88 | 7.72 |
| $R_{Bragg}$ | 11.59 | 13.31 | 4.33 |
| $S$ | 1.79 | 1.559 | 1.1 |

Note: For $M$ and $\langle \epsilon^2 \rangle^{1/2}$, subscripts 11, 22 and 33 are along $a$, $b$ and $c$ axis directions, respectively. The fitting index of Rietveld analysis: $R_{wp}$=weighted pattern factor, $R_p$=pattern factor, $R_{Bragg}$=Bragg factor, $S$=goodness of fit.

dimension are affected markedly by different material processing methods. In addition, the micro-strain of annealed and melt-spun alloys is much smaller than that of as-cast alloy.

### 3.2. Microstructure

Fig. 2(a–c) shows the SEM micrographs of the three alloys. It can be seen that the as-cast alloy assumes a typical dendrite structure. After being annealed the alloy changes to an equiaxed structure. The melt-spun alloy is characterized by a very fine cellular structure. The result that no secondary phase is observed in all these three alloys is in good agreement with the XRD analysis.

Fig. 3 shows the composition of La, Mn and Fe for sites every 1 μm apart along a straight line on the surface of these alloys by EDS analysis. The results indicate that the distribution of La, Mn and Fe in the annealed and melt-spun alloys is much more uniform in comparison with that of the as-cast alloy. This means that the annealing and melt-spinning process effectively improves the compositional homogeneity of the alloy.

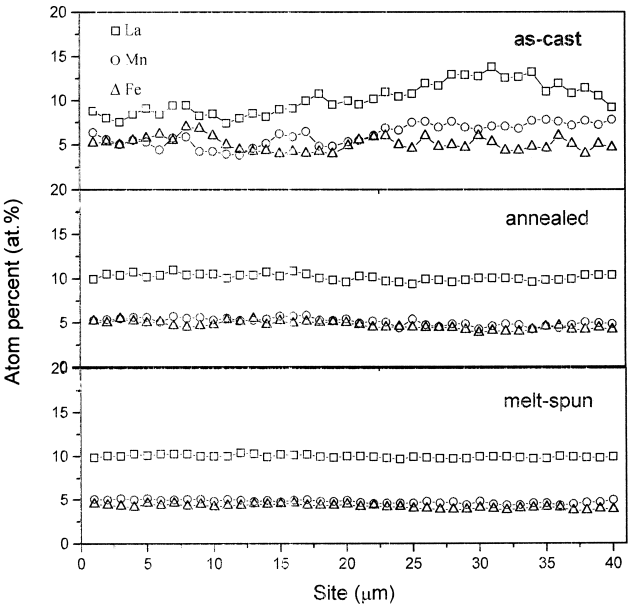


Fig. 3. EDS analysis results of La, Mn and Fe distribution in $MlNi_{4.1}Mn_{0.35}Al_{0.3}Fe_{0.25}$ alloys.

### 3.3. Electrochemical properties

Table 2 shows the electrochemical properties of the three alloys. It can be seen that the as-cast alloy needs only three cycles to reach its maximum capacity of 310 mA h $g^{-1}$. The activation cycles of the annealed alloy increases to six cycles and its discharge capacity decreases to 298.5 mA h $g^{-1}$, while the melt-spun alloy needs eight activation cycles with a maximum discharge capacity of 305 mA h $g^{-1}$.

As shown in Fig. 4, the discharge potential plateaus of both the annealed and melt-spun alloys are flatter and a little lower (more positive) than that of the as-cast alloy, which can be ascribed to the more homogeneous composition of the alloy after annealing and rapid quenching. In addition, the width of discharge potential plateaus of the annealed and melt-spun alloy are slightly shorter, leading to a slightly lower discharge capacity.

From Table 2, it is also found that the high-rate dischargeability of the melt-spun alloy is slightly lower

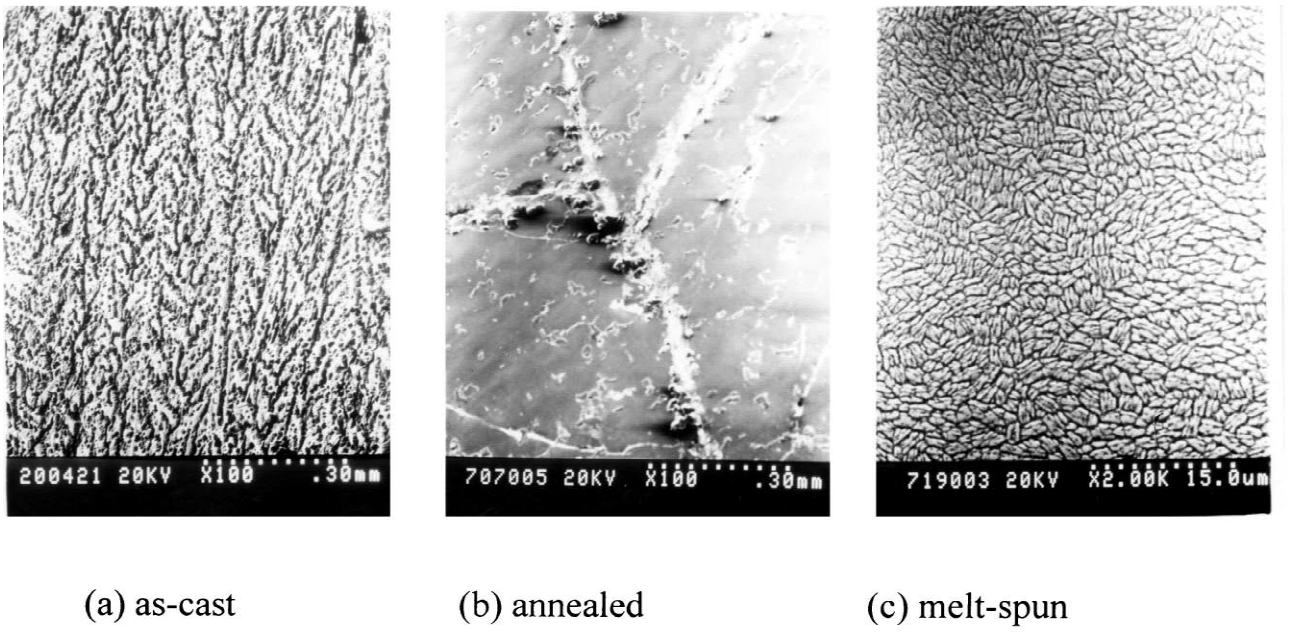


Fig. 2. SEM images of $MlNi_{4.1}Mn_{0.35}Al_{0.3}Fe_{0.25}$ alloys prepared by three different methods. (a) As-cast, (b) annealed, (c) melt-spun.

Table 2
Electrochemical properties of $MlNi_{4.1}Mn_{0.35}Al_{0.3}Fe_{0.25}$ alloys (25°C)

| Alloy | Discharge capacity (mA h $g^{-1}$) | Activation number ($n$) | Capacity retention rate (%) after 300 and 500 cycles | | High-rate dischargeability (%) at different discharge currents (mA $g^{-1}$) | | |
|---|---|---|---|---|---|---|---|
| | | | $S_{300}$ | $S_{500}$ | 300 | 600 | 900 |
| As-cast | 310.5 | 3 | 64.5 | 45.1 | 88.9 | 72.9 | 54.5 |
| Annealed | 298.5 | 6 | 67.6 | 61.2 | 73.4 | 53.0 | 22.2 |
| Melt-spun | 305.4 | 8 | 75.9 | 69.2 | 85.6 | 67.4 | 31.3 |

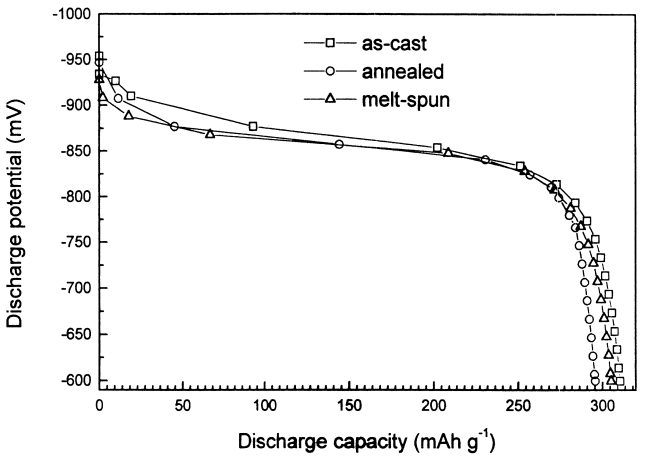


Fig. 4. The discharge potential curves of $MlNi_{4.1}Mn_{0.35}Al_{0.3}Fe_{0.25}$ alloys.

than that of the as-cast alloy, but higher than that of annealed alloy. At the discharge rate of 300 mA $g^{-1}$, the high-rate dischargeability of the as-cast alloy reached 88.9%, and was only 85.6 and 73.4% for the melt-spun and annealed alloy, respectively. When the discharge current is higher than 600 mA $g^{-1}$, the high-rate dischargeability of the annealed and melt-spun alloy drops to a much lower value than that of the as-cast alloy.

As shown in Fig. 5, the as-cast Co-free alloy shows a rather poor cycling stability. Its discharge capacity is reduced to less than half of the initial value after 500 cycles ($S_{500}$=45.1%) at the charge/discharge current of 300 mA $g^{-1}$, while the cycling stability of the alloy is dramatically improved by an additional annealing treatment or rapid quenching. The capacity retention rate ($S_{500}$) of the annealed alloy goes up to 61.2%, and increases to 69.3% for the melt-spun alloy.

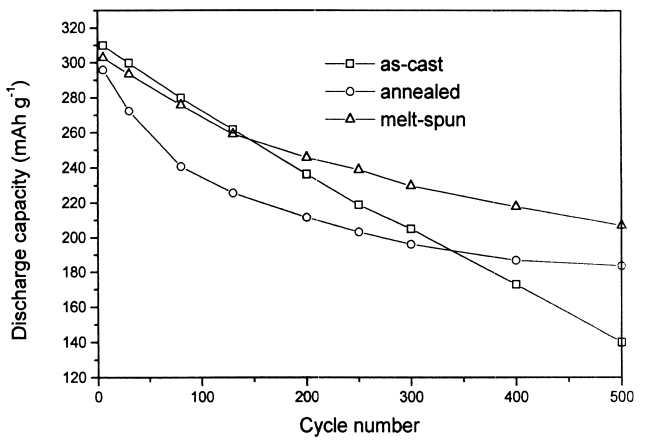


Fig. 5. Cycling stability of $MlNi_{4.1}Mn_{0.35}Al_{0.3}Fe_{0.25}$ alloys (at 300 mA $g^{-1}$).

Fig. 6 shows the optical micrographs of the polished surface of the three alloy electrode samples after 500 cycles. It can be seen that the pulverized alloy particles with different size (white parts) are embedded in the Cu powder (black parts). Since the three alloys have the same composition, the obvious difference in particle size of the alloys after cycling indicates that the pulverization property of the alloys depends strongly on the alloy microstructure, which changes with alloy preparation method. The as-cast alloy with a dendrite structure pulverizes rather readily. The annealed alloy of equiaxed structure has a lower pulverizing rate compared to the as-cast alloy, while the alloy prepared by melt-spinning with a very fine cellular structure acquires high resistance to pulverization. It is well accepted that the higher pulverizing rate of the alloy, which causes a rapid increase in reaction surface area, is of benefit to the initial activation and high-rate dischargeability of alloys, but also suffers from more serious corrosion, which leads to a faster capacity decay at the new surface of alloy in contact with the alkaline electrolyte. While the annealed alloy and especially the melt-spun alloy both have a higher resistance against pulverization therefore a big improvement in the corrosion stability and cyclic endurance, yet their activation rate and high-rate dischargeability are both decreased somewhat.

In addition to the microstructure and pulverization property, the homogeneity of alloy composition is also very important for the corrosion resistance and cycling stability. As the annealed and melt-spun alloys both have much more homogeneous composition than the as-cast alloy (as seen in Fig. 3), their corrosion resistance and cycling stability are improved by the reduction of oxidation of La, Mn, Fe and the dissolution of Mn from the alloy into KOH solution.

Among the Co-free $MlNi_{4.1}Mn_{0.35}Al_{0.3}Fe_{0.25}$ alloys prepared by three different methods in this work, the melt-spun alloy has the best cycling stability ($S_{500}$= 69.3%), a reasonably high discharge capacity (305 mA h $g^{-1}$) and 1C rate dischargeability (85.6%), owing to its

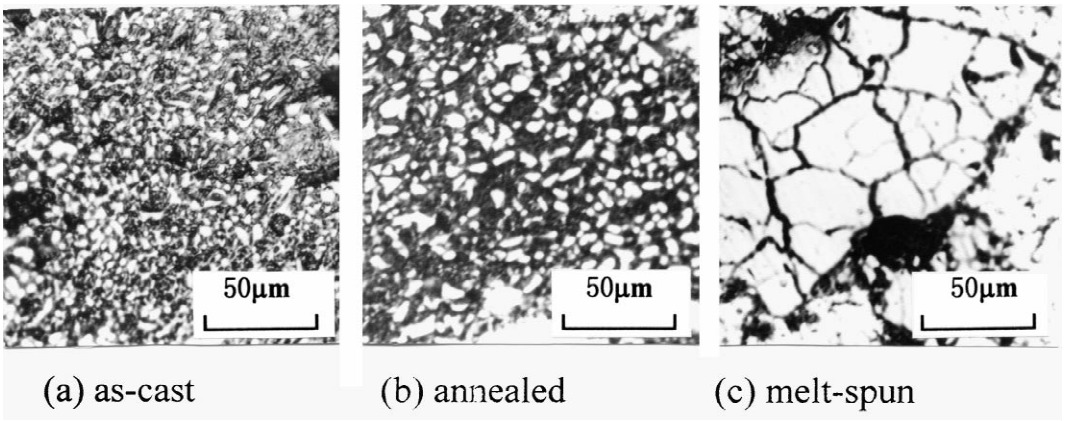


Fig. 6. Optical micrographs of the polished surface for the three alloys after 500 cycles. (a) As-cast, (b) annealed, (c) melt-spun.

higher pulverization resistance and highly homogenized composition. It is thus clear that the melt-spinning process is an effective method to improve the cycling stability of the Co-free alloy without much detrimental effect on the other electrochemical properties of the alloy. It can be a good candidate for the low-cost negative electrode materials for Ni/MH batteries. For the improvement of the activation property and high-rate dischargeability of the melt-spun Co-free alloy, some further experiments in surface treatment are required.

## 4. Conclusions

Cobalt-free $MlNi_{4.1}Mn_{0.35}Al_{0.3}Fe_{0.25}$ alloys were prepared by three different processing methods, and their microstructure and electrochemical properties were examined and compared. It is found that the microstructure and electrochemical properties of the alloys are influenced greatly by the alloy preparation methods. The as-cast alloy has a dendrite structure, high pulverizing rate and noticeable element segregation, which all result in a poor cyclic endurance. Annealing treatment changes the alloy to an equiaxed structure, lowers the pulverizing rate and improves greatly the composition homogeneity, leading to a marked improvement in cycling stability. The alloy prepared by melt-spinning is characterized by a very fine cellular structure, highly homogenized composition, high resistance against pulverization, good cycling stability ($S_{500}$=69.3%), a reasonably high capacity (305 mA h $g^{-1}$) and good 1C rate dischargeability (85.6%). On the other hand, the activation rate and high-rate dischargeability of the annealed and melt-spun alloys are somewhat lower in comparison with the as-cast alloy. The melt-spun cobalt-free $MlNi_{4.1}Mn_{0.35}Al_{0.3}Fe_{0.25}$ alloy is a promising candidate for the low-cost negative electrode materials for Ni/MH batteries.

## Acknowledgements

This work is supported by the National Advanced Materials Committee of China (project no. 863-715-004-0060).

## References

[1] F. Meli, A. Züttel, L. Schlapbach, J. Alloys Comp. 231 (1995) 639–644.
[2] W.K. Hu, H. Lee, D.M. Kim, S.W. Jeon, J.Y. Lee, J. Alloys Comp. 268 (1998) 261–265.
[3] W.K. Hu, D.M. Kim, K.J. Jing, J.Y. Lee, J. Alloys Comp. 269 (1998) 254–258.
[4] K. Yasuda, J. Alloys Comp. 253–254 (1997) 621–625.
[5] A. Züttel, D. Chartouni, K. Gross, P. Spatz, M. Bächler, F. Lichtenberg, A. Fölzer, N.J.E. Adkins, J. Alloys Comp. 253–254 (1997) 626–628.
[6] F. Lichtenberg, U. Köhler, A. Fölzer, N.J.E. Adkins, A. Züttel, J. Alloys Comp. 253–254 (1997) 570–573.
[7] N. Higashiyama, Y. Matsuura, H. Nakamura, M. Kimoto, M. Nogami, I. Yonezu, K. Nishio, J. Alloys Comp. 253–254 (1997) 648–651.
[8] C.J. Li, X.L. Wang, C.Y. Wang, J. Alloys Comp. 293–295 (1999) 742–746.
[9] T. Sakai, H. Yoshinaga, H. Miyamura, H. Ishikawa, J. Alloys Comp. 180 (1992) 37–54.
[10] T. Sakai, H. Miyamura, N. Kuriyama, H. Ishikawa, I. Uehara, Z. Phys. Chem. 183 (Suppl. 333-346) (1994) 1373–1386.
[11] R. Mishima, T. Sakai, N. Kuriyama, H. Ishikawa, I. Uehara, J. Alloys Comp. 192 (1993) 176–178.